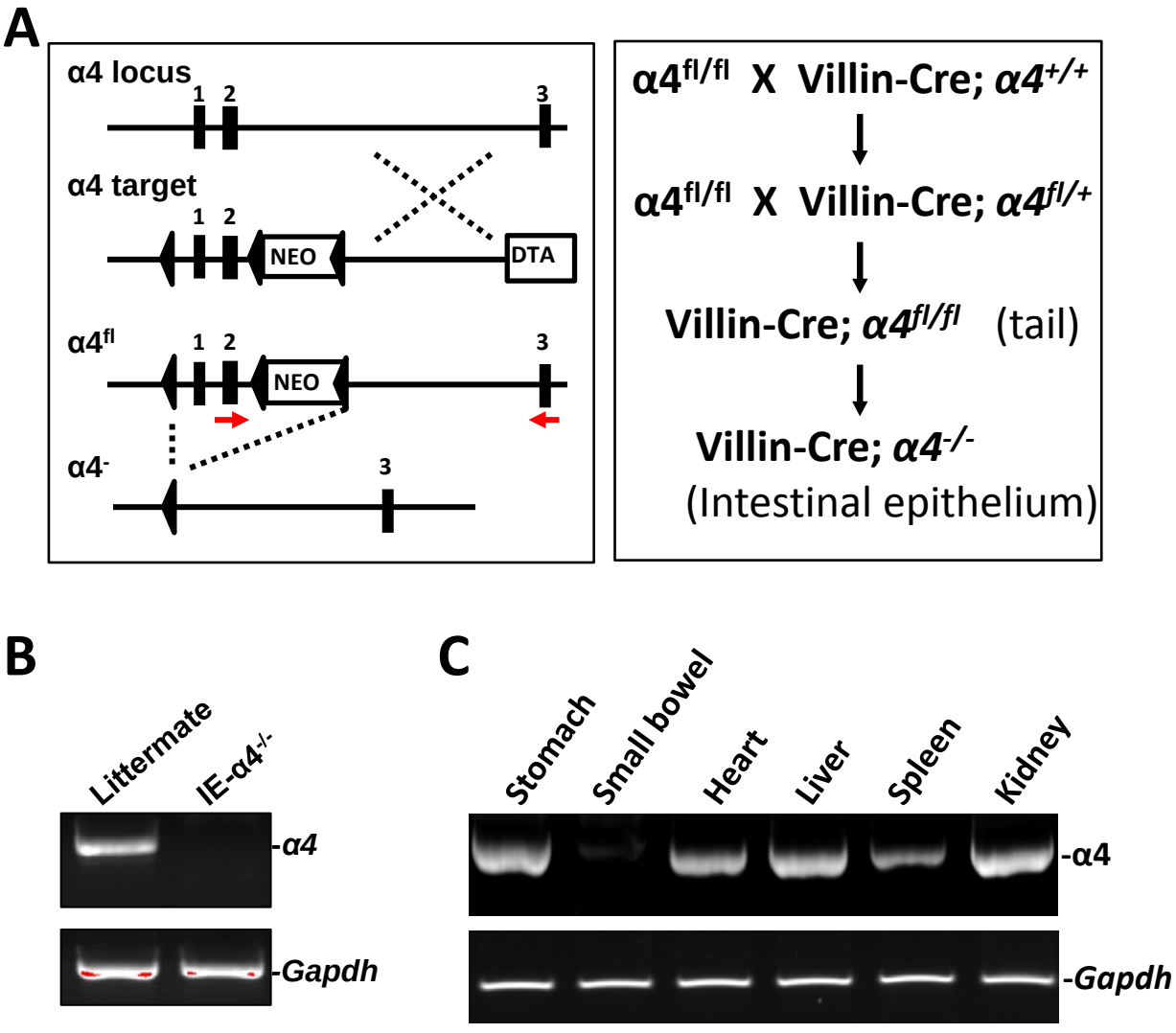


**Supplementary Figure 1:** Strategy for generation of IE-α4$^{-/-}$ mice and expression of α4 in other organs. **(a)** Schematic of the complete exon-intron orientation of the α4 locus and magnification of the NEO-containing exon. **(b)** Levels of α4 mRNA in the small intestinal mucosa obtained from littermate and IE-α4$^{-/-}$ mice as measured by RT-PCR analysis. **(c)** Levels of α4 mRNA in stomach mucosa, small intestinal mucosa, heart, liver, spleen, and kidney in IE-α4$^{-/-}$ mice.

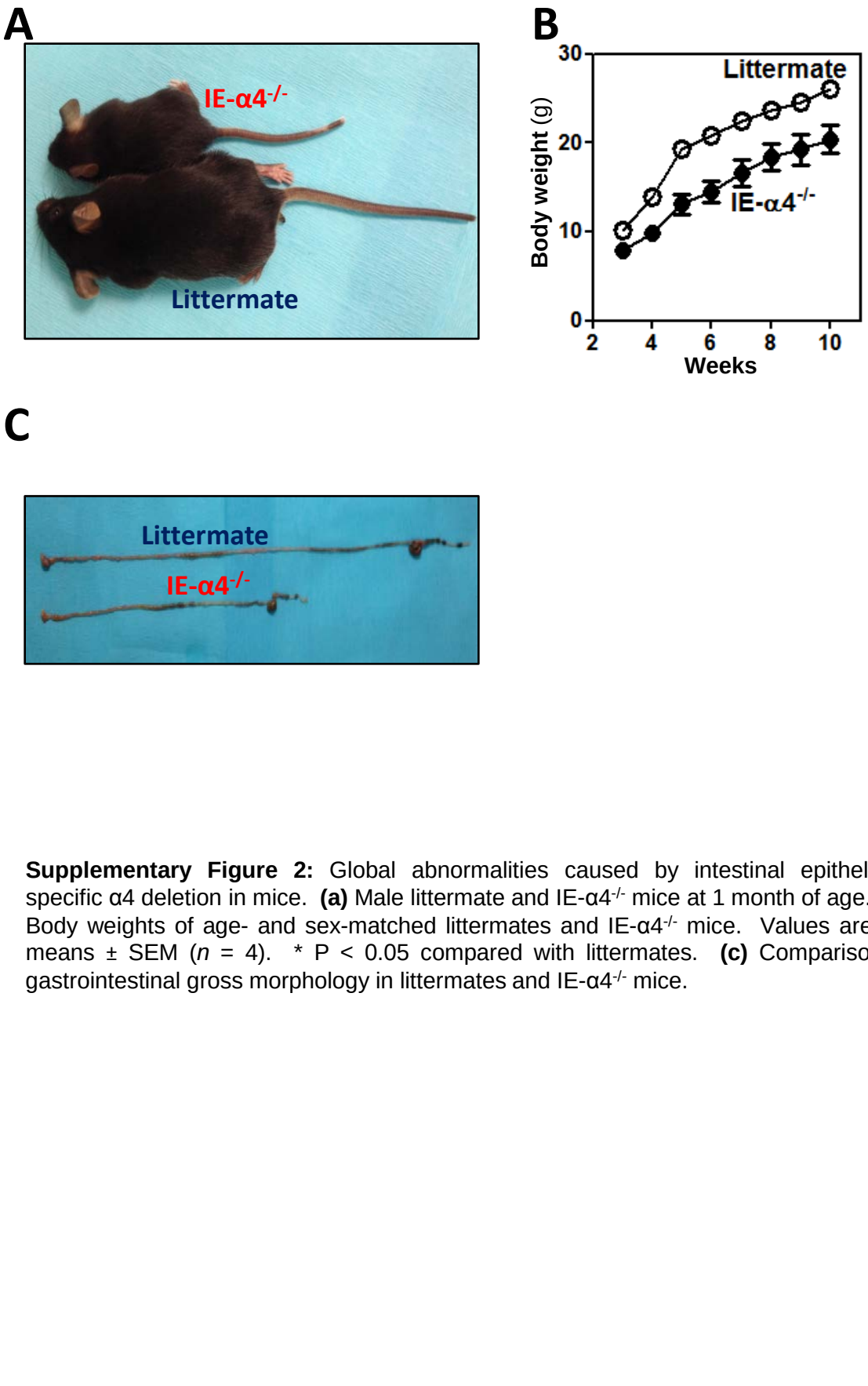


**Supplementary Figure 2:** Global abnormalities caused by intestinal epithelium-specific α4 deletion in mice. **(a)** Male littermate and IE-α4$^{-/-}$ mice at 1 month of age. **(b)** Body weights of age- and sex-matched littermates and IE-α4$^{-/-}$ mice. Values are the means ± SEM ($n$ = 4). * $P < 0.05$ compared with littermates. **(c)** Comparison of gastrointestinal gross morphology in littermates and IE-α4$^{-/-}$ mice.

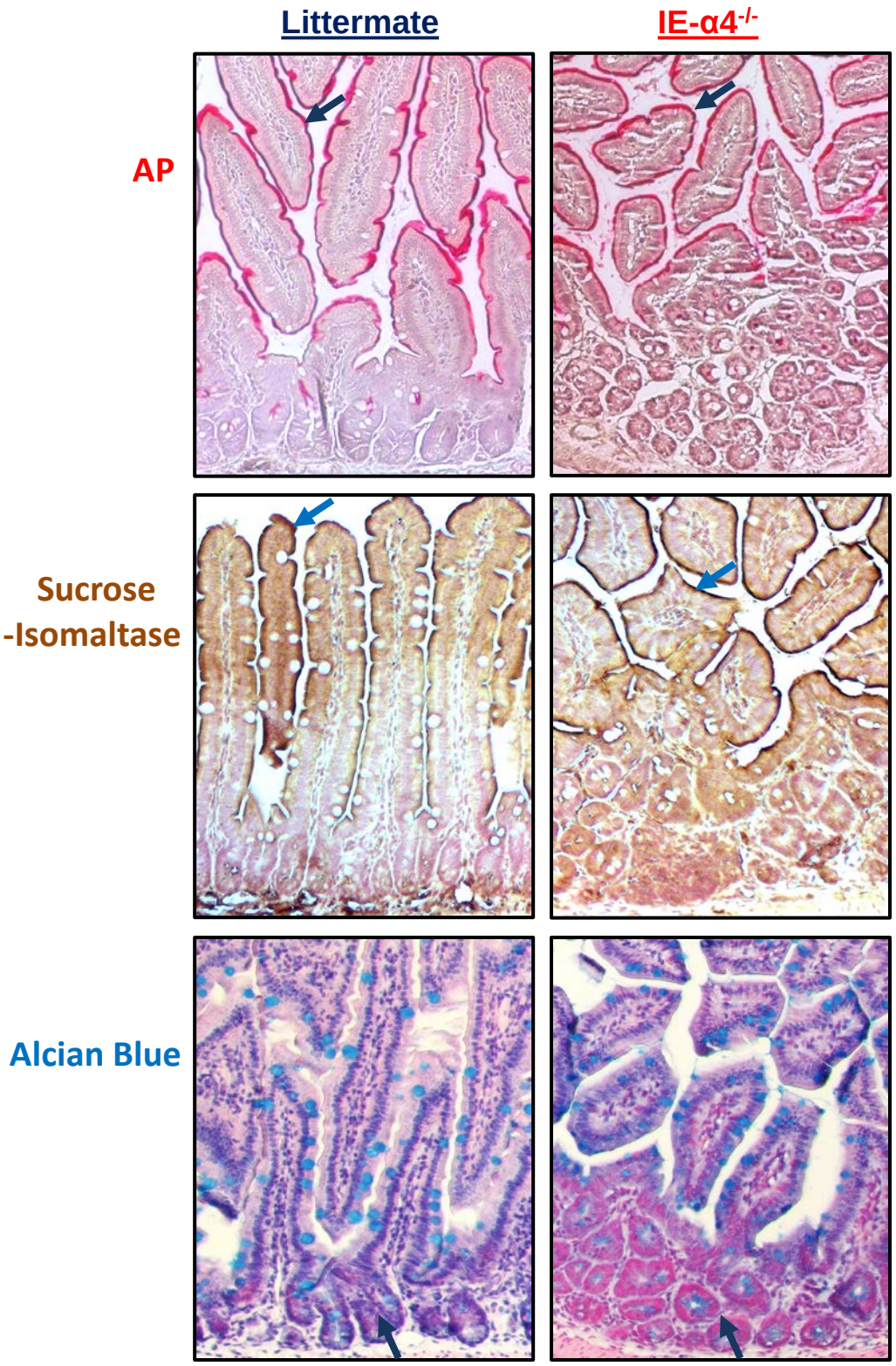


**Supplementary Figure 3:** Immunochemical staining of brush border membrane proteins and goblet cells in the small intestinal mucosa. Alkaline phosphatase (AP) and sucrose-isomaltase are shown as red and brown, respectively (arrow). Goblet cells were examined by alcian blue (blue, arrow). Sections were counterstained with nuclear fast red.

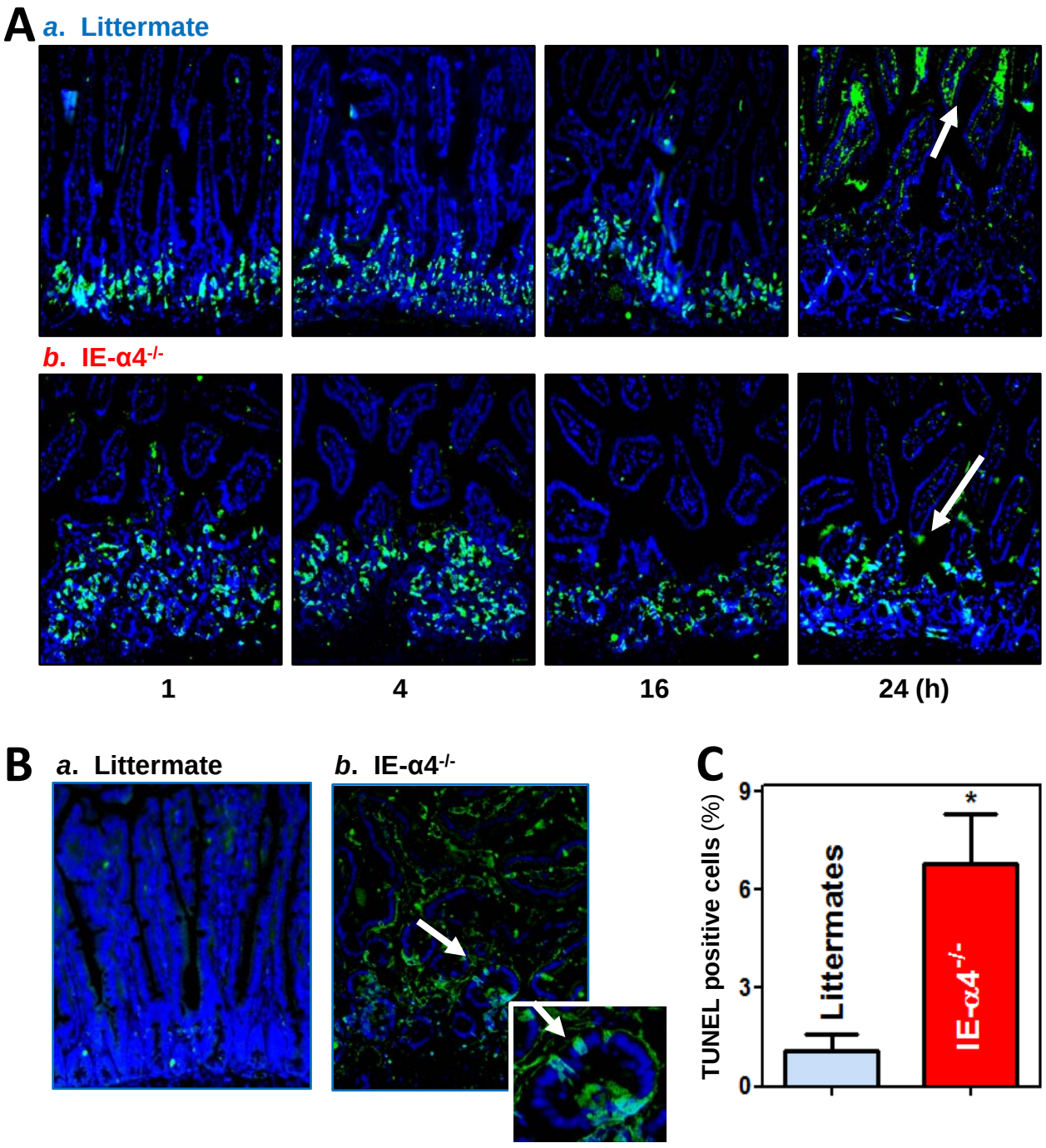


**Supplementary Figure 4:** α4 deletion inhibits cell migration and induces epithelial cell death in the small intestine. **(a)** Changes in the rate of epithelial cell migration in the small intestinal mucosa of littermate (***a***) and IE-α4$^{-/-}$ (***b***) mice. Mice were injected with BrdU, and the mucosal tissues were harvested at the times indicated. **(b)** Epithelial cell death as examined by TUNEL staining (shown as green) in the small intestine of littermate (***a***) and IE-α4$^{-/-}$ (***b***) mice. **(c)** Summary of TUNEL-positive cells in mucosa prepared as described in (b) ($n$ = 6). * $P < 0.05$ compared with littermates.

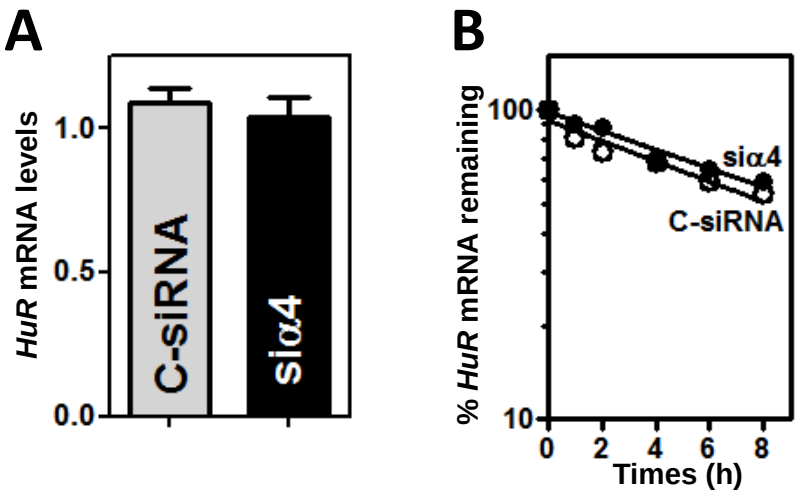


**Supplementary Figure 5:** α4 silencing fails to alter levels and stability of the *HuR* mRNA. **(a)** Steady-state levels of *HuR* mRNA 48 h after transfection with siα4 or C-siRNA. **(b)** Half-life of the *HuR* mRNA in cells described in (a). The levels of *HuR* mRNA were examined at different times after administration of actinomycin D. Values are the means ± SEM of data from triplicate experiments.

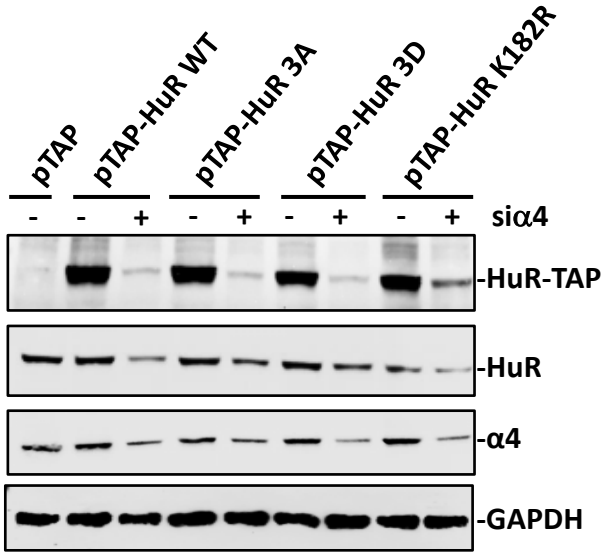


**Supplementary Figure 6**. The relative stability of each of HuR-TAP mutants after α4 silencing in cultured IECs. Cells were co-transfected with siα4 and pTAP-HuR WT (wild-type HuR-TAP), pTAP-HuR3A (carrying three non-phosphorylatable mutations, S88A, S100A, T118A), pTAP-HuR3D (carrying three non-phosphorylatable mutations, S88D, S100D, T118D), or pTAP-HuR K182R. The levels of HuR-TAP were examined 48 h after the transfection by Western blotting analysis.